Study on H-Infinity control for LAMOST main axes

Wangping Zhou[1,2], Xinqi Xu[1], Zhiming Dong[1,2]

1. National Astronomical Observatories /Nanjing Institute of Astronomical Optics & Technology，

Chinese Academy of Sciences，Nanjing 210042

2. Graduate School of the Chinese Academy of Sciences, Beijing 100049

ABSTRACT

The workshop test of mount drive for Large Sky Area Multi-Object Fiber Spectroscopic Telescope (LAMOST) was completed in June of 2005. Now the giant mount has just been erected on Xinglong station, and is due to test in the summer of 2006. LAMOST mount mechanism features friction drive on both axes, and oil pad is employed specifically for the azimuth. For further improving the tracking accuracy in worse surroundings some nonlinear phenomena in the drive chain have to be addressed. Moreover, external uncertainties on Xinglong site, wind buffeting in particular, could affect load variation on the drive. The control system parameters would change with time, thus eventually degrade the tracking performance. All these reasonable assumptions call for a more robust controller than conventional PID approach to cope with. This is where H-Infinity controller comes in. This paper focuses on the mount drive of LAMOST by using H-Infinity technique and comparison with the PID servo. The load disturbance rejection is discussed, as well as transmission rigidity improvement is analyzed. Study and simulation are done in Matlab. The model test in our friction drive lab is presented.

Keywords: H-Infinity, PID, control system, LAMOST

1．INTRODUCTION

Friction drive is frequently utilised in main axes drive system of contemporary astronomical telescopes, and the LAMOST telescope is no exceptional. Main advantage of friction drive is in the positioning accuracy, which is not affected by backlash like conventional gear drive systems. Friction drive is a kind of novel drive settings, which demands for better performance of control to achieve high precision angular position. However, since the friction torque between the azimuth axis and axletree is nonlinear to some extend, the contact between the driving wheel and passive wheel cannot be idealized, and there's not an extremely glabrous contact surface along with non-zero radical flop, and no immense transmission rigidity that all together make an alterable disturbance torque and hence affect the tracking precision. Among these factors, friction undoubtedly is the dominating one. Paper [1] refers to a kind of robust nonlinear friction compensation method to restrain oscillating of stable limit cycles. Using mathematic model to analyse friction phenomena, paper [2] proposes the back-stepping sliding mode controller to improve tracking performance in the sliding and pre-sliding phase. It is inevitable to establish mathematical model of friction torque when using friction compensation based on friction model, and to introduce model output acting as compensation signal to counteract friction torque. But in practice, it is very difficult to form precise mathematical model. And if the model is imprecise, the compensation torque will be hard to avoid over responding or insufficient. Paper [3] mentions a kind of robust nonlinear control based on Lyapunov direct method, through introducing robust compensation to counteract the friction moment,

Optomechanical Technologies for Astronomy, edited by Eli Atad-Ettedgui, Joseph Antebi, Dietrich Lemke,
Proc. of SPIE Vol. 6273, 627333, (2006) · 0277-786X/06/$15 · doi: 10.1117/12.671107

meanwhile, adopting nonlinear gain to conquer parameter uncertainty. Upper bound replacing precise math model makes this method a feasible approach. In this paper, we first give a brief statement of friction, and the nonlinear wind disturbance will be analysed. Second, we will present the on line friction compensation with PID controller. At last, a robust H_∞ control method by taking nonlinear disturbances as model oscillations will be presented in detail.

2. FRICTION MODEL

The friction mechanism applied in main axes structure of astronomical telescopes can generally be simplified as a pair of wheels contacted along a common cylinder generatrix. One wheel in the pair is driving wheel and the other driven wheel with radially applied force to make a close contact between the two wheels. The friction in the contact area between the driving wheel and the driven wheel features complex motions such as pre-sliding displacement, break-away, and stick-slip etc, thus making friction an important aspect in high quality servo systems. Model-based friction compensation schemes resort to a suitable friction model to predict the friction without adopting high gain control loops. The representative LuGre friction model has been applied to many friction compensation control systems. It is derived from the bristle model assuming that the friction interface is thought as a contact between bristles. The friction force can be represented with nonlinear internal friction dynamics as follows [4,5]:

$$F = \sigma_0 z + \sigma_1 \dot{z} + \sigma_2 \dot{\theta} \tag{1}$$

$$\dot{z} = \dot{\theta} - \frac{|\dot{\theta}|}{g(\dot{\theta})} z \tag{2}$$

$$\sigma_0(\dot{\theta}) = F_C + (F_S - F_C) e^{-(\dot{\theta}/\dot{\theta}_s)^2} \tag{3}$$

where z and θ are the internal states of friction model and the position of the system respectively, σ_0 and σ_1 are terms of the bristle model, σ_2 is vicious friction coefficient respectively, F_C and F_S represent Coulomb friction and static friction respectively, $\dot{\theta}_S$ denotes Streibeck velocity, and $g(\dot{\theta})$ describes the Streibeck behaviour. Figure 1 shows the friction torque against the corresponding velocity by simulation in Matlab.

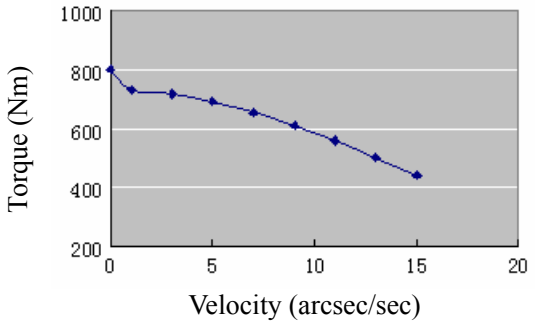

Fig.1 friction against velocity

3. FRICTION COMPENSATION

Figure 2 shows LAMOST block diagram of drive transfer functions, where V_{da} and V_a denote input and control voltage respectively, K is voltage magnifying coefficient, R_g represents output resistance of amplifier, R_{a1} and R_{a2} are armature resistances of motor 1 and motor 2 respectively, I_a is armature current of motor, K_{t1} and K_{t2} denote torque coefficients of motor 1 and 2 respectively, M_u is motor torque, M_b represents load torque, J is moment of inertia that is converted to motor axis, $\dot{\theta}_m$ is motor angular velocity, $\dot{\theta}$ denotes the driven wheel's angular velocity, N is the ratio between motor and the driven wheel, V_e represents the measured feedback velocity, F is viscous coefficient, K_{e1} and K_{e2} denote the two motors' counter electromotive force coefficient respectively, K_{tg} is tachometer transfer coefficient.

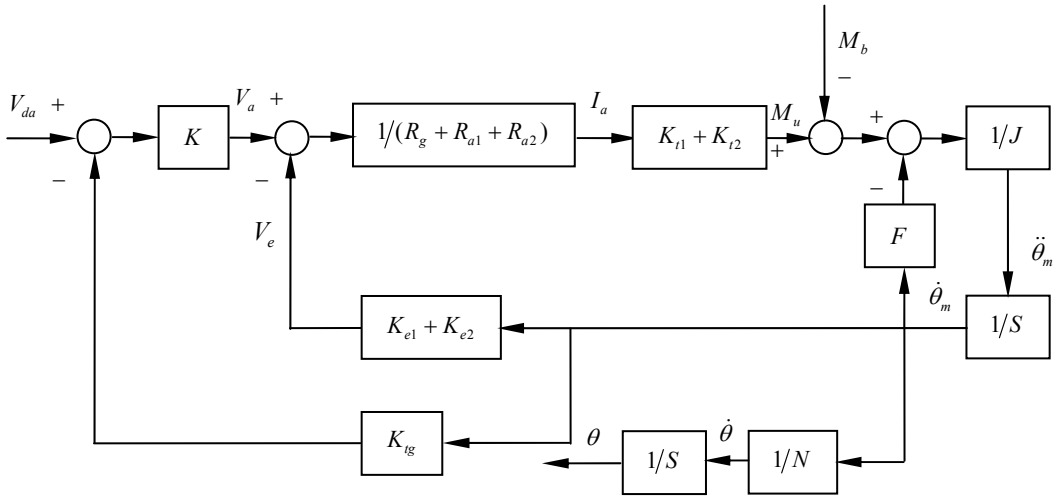

Fig.2 Block diagram of drive transfer function

From figure 2, the states could be formed as follows:

$$\ddot{\theta}_m(t) = -\frac{K_t(KK_{tg}+K_e)+FR}{RJ}\dot{\theta}_m(t) + \frac{K_tK}{RJ}V_{da}(t) \tag{4}$$

Formula (4) describes the plant (P) under control. Due to the load torque cannot be measured directly, it needs to differentiate and analyse the model to get an approximation.

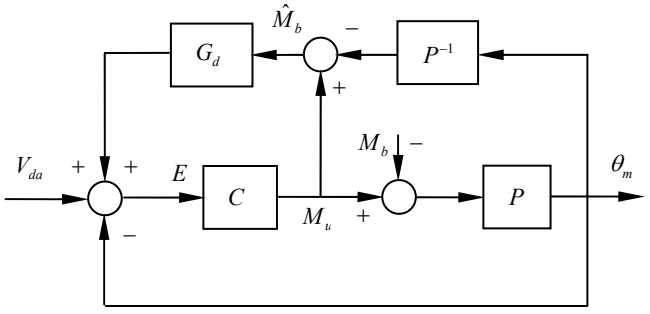

Fig.3 Block diagram of feedforward friction compensation

From figure 3, we get:

$$M_b(s) = M_u(s) - P^{-1}(s)\theta(s)$$

By replacing measured control signal M_u and putting system output θ_m into above formula, it is easy to get the estimated value of $\hat{M}_b$. Feedforward compensation design scheme consists in finding controller G_d that counteracts friction torque M_b based on the estimated $\hat{M}_b$. In figure 3, C is the feedback controller transfer function, P denotes the plant just formulated by formula (4). From the block diagram:

$$E(s) = V_{da}(s) - \theta_m(s) - G_d(s)\hat{M}_b \tag{5}$$

$$\theta_m(s) = P(s)[C(s)E(s) - M_b(s)] \tag{6}$$

The system transfer function then could be described by:

$$\theta_m(s) = \frac{P(s)C(s)V_{da}(s) + P(s)C(s)G_d(s)\hat{M}_b(s) - P(s)M_b(s)}{1 + P(s)C(s)} \tag{7}$$

Once the feedforward transfer function G_d is determined by C^{-1} and assuming that $\hat{M}_b$ almost equals to M_b, the affect of friction load torque could be approximately compensated.

Another compensation approach is applying aforementioned friction model. Assuming that the parameters σ_0, σ_1 and σ_2, and the function g in the friction model are known. Since the state z is not measurable, it is necessary to design an observer for estimating the friction force. The nonlinear friction observer can be described by:

$$\frac{d\hat{z}}{dt} = \dot{\theta}_m - \frac{|\dot{\theta}_m|}{g(\dot{\theta}_m)}\hat{z} - ke \quad k > 0 \tag{8}$$

$$\hat{F} = \sigma_0\hat{z} + \sigma_1\frac{d\hat{z}}{dt}\sigma_2\dot{\theta}_m \tag{9}$$

where $e = V_{da} - \theta_m$ is the position error and V_{da} is the desired reference which is assumed to be twice differentiable. ke is a correction term from the position error in the observer. The position errors of PID controller with tracking speed 1arcsec/s based on LuGre friction model are shown in figure 4 and 5.

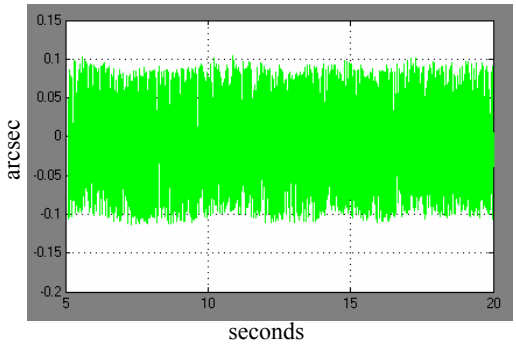

Fig.4 Position error curve of Azimuth (1arcsec/s)

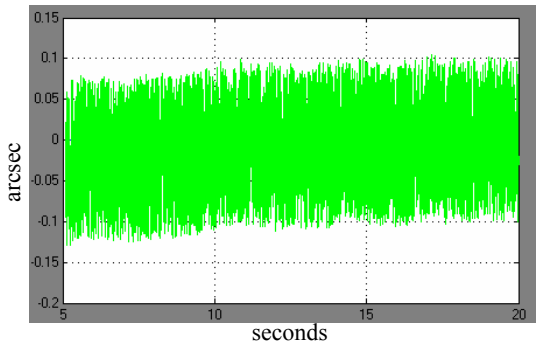

Fig.5 Position error curve of Altitude (1arcsec/s)

4. WIND DISTURBANCE

The Alt-Az mount of LAMOST carries the reflecting Schmidt plate which consists 24 pieces of hexagonal sub-mirrors with the diameter about 5m as a whole. Especially the mount is erected on Xinglong mountain. So wind will be the uppermost factor of disturbances which affect the performance of the mount movement. To reject wind disturbance, it needs first to found a wind model which could predict the disturbance. A common used wind model is Davenport spectral density model which separates the torque of wind disturbance into two parts [6]: one is the DC part of the wind which brings a constant torque, the other is a time-varying part. The DC part can be described by

$$T_{const} = C_T qAD \tag{10}$$

where

C_T is wind torque coefficient, $q = 1/2\,\rho v^2$ denotes the dynamic pressure, ρ is density of air, v denotes wind velocity, A represents the contact area and D is the radius of the axis which vertical to A. The time-varying part could be formed as follows:

$$T_{vary} = 4K_o v^2 (\rho v C_T AD)^2 \frac{(fK_a/v)^2}{f[1+(fK_a/v)^2]^{\frac{4}{3}}} \tag{11}$$

where $K_o = [0.4 \Big/ \ln(\frac{z_r}{z_o})]^2$, z_o denotes surface roughness length of local terrain, z_r is reference height, f represents frequency and K_a is terrain roughness constant.

5. H_∞ CONTROL

Almost all control systems in practical engineering consist uncertain character for a variety of reasons. This uncertain character generally could be divided into two parts: one is outer uncertainty such as disturbance etc; the other is called inner uncertainty like measure of error, un-modelling dynamics of the control object and so on. So it is difficult to describe the practical engineering-oriented systems with precise mathematical model. The existing Lyapunov stable theory based on accurate differential equation with finite dimensions regards this system uncertainty as tiny disturbance at initial conditions of the differential equation. It uses the stability of standard system to ensure that the actual system responds stably to the initial conditions caused by those uncertainties. But this method differs greatly from the instance in real engineering. What is more, it is incapable to quantitatively grasp the impact on the performance of system caused by uncertainties. Fortunately H-infinity control theory offers feasible techniques to treat with these uncertainties. As for LAMOST drive control system, there is also two kinds of uncertainties: wind disturbance belongs to outer uncertainty and friction torque is inner uncertainty.

a model uncertainty

The alterable load torque (main of it is friction torque) and other nonlinear affects could be considered as system uncertainty. Thus, the transfer function $P_0(s)$ of standard system along with the bound $r(s)$ of unknown error function $\Delta P(s)$ describes the real mount drive system. There are several structures of model uncertainty. Both standard system model and bound function of uncertainty are needed no matter what structure is selected. In this paper,

multiplicative uncertainty model is chosen. Figure 6 shows multiplicative uncertainty model:

$$P(s) = [1 + \Delta P(s)W(s)]P_0(s), \quad \left\|\Delta P(s)\right\|_\infty < 1 \tag{12}$$

where $W(s)$ denotes bound function of uncertainty model $\Delta P(s)$.

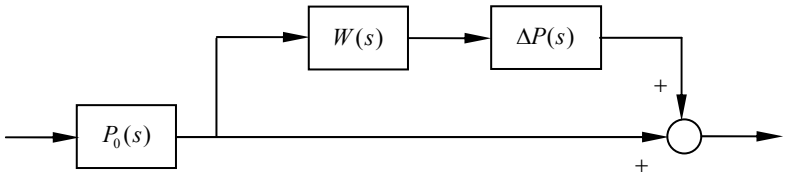

Fig.6 Block diagram of multiplicative uncertainty

b disturbance rejection

With regard to SISO system, the H_∞ norm of transfer function $P(s)$ could be described by:

$$\left\|P\right\|_\infty = \sup_\omega \left|P(j\omega)\right| \tag{13}$$

Above function could be explained as the maximum amplitude caused by unit impulse response. Once the frequency response of disturbance is determined, system output $\theta(t)$ then could be expressed as transfer function $P(s)W(s)$ responding to unit impulse. In order to reject disturbance response, it needs (14) to come into existence with regard to a certain positive numerical value γ.

$$\left\|\hat{\theta}(s)\right\|_\infty \le \left\|P(s)W(s)\right\|_\infty < \gamma \tag{14}$$

Note that $W(s)$ is a penalty function. It in fact is the model of disturbance in problems such as disturbance rejection. The upper bound of disturbance may be taken as penalty function as long as it could be estimated when the frequency characteristics of disturbance are ambiguous. In fact, as shown in figure 7, if the disturbance satisfies the following condition:

$$\left|\hat{d}(j\omega)\right| \le \left|W(j\omega)\right|, \quad \forall \omega \in R \tag{15}$$

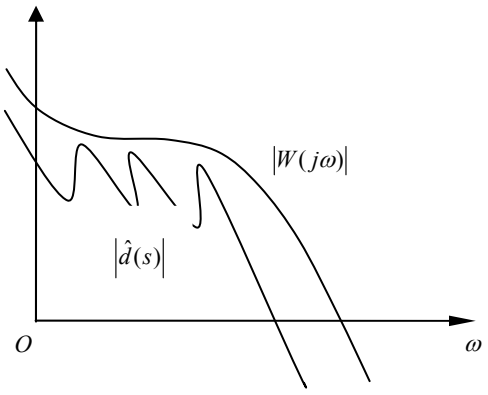

Fig.7 Penalty function

the maximum amplitude of output frequency response caused by disturbance will less than γ as long as (14) holds.

c robust control theory

From the two former parts of this section, both model uncertainty and disturbance rejection can be transformed into determining penalty function. So the next question is how to deal with these penalty functions as far as control is concerned? To begin this, the stable theory is indispensable. First, we would like to introduce the famous small gain theorem with regard to the system shown in figure 8, where $M(s)$ is the already known system, $\Delta(s)$ denotes unknown oscillating. Both $M(s)$ and $\Delta(s)$ are the analytic rational function in the closed right s-plane.

Theorem: Assuming that the uncertain oscillating is bound and satisfied with $\|\Delta(s)\|_\infty \le 1$, the sufficient and necessary condition of robust stable system is $\|M(s)\|_\infty < 1$.

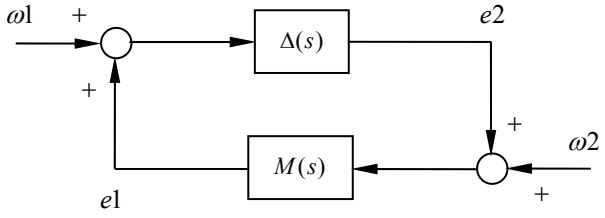

Fig.8 Block diagram of small gain theorem

Both the closed loop system of model uncertainty and disturbance rejection should be standardized like the form shown in figure 8 according to small gain theorem. Through loop shaping, as for model uncertainty, the closed-loop system $M(s)$ could be shaped as $W(S)P(s)C(s)/[1+P(s)C(s)]$, where $P(s)$ and $C(s)$ equal to P and C in figure 3 respectively. So the robust stable condition can be described by:

$$\left\| \frac{W(s)P(s)C(s)}{1+P(s)C(s)} \right\|_\infty \le 1 \tag{16}$$

As far as disturbance rejection is concerned, the robust stable condition then can be expressed as:

$$\left\| \frac{W(s)}{1+P(s)C(s)} \right\|_\infty \le 1 \tag{17}$$

There is only one unknown variable $C(s)$ in formulas (16) and (17). So they are solvable in theory. At present, the two main approaches to get the controller $C(s)$ are Riccati Equations and Linear Matrix Inequalities (LMI). The approach based on Riccati equations transforms existing conditions for an H_∞ controller into two Riccati equations and a spectral radius condition, and the set of all H_∞ controllers is parameterized using the unique stabilizing solutions to the Riccati equations with free parameter Q, a real-rational transfer matrix with an H_∞ norm less than a specified number. LMI changes existing conditions into three linear matrix inequalities. The set of all H_∞ controllers is parameterized using positive definite solutions to the linear matrix inequalities, which form a convex set. There will be a set of H_∞

controllers corresponding to the positive definite matrices. A state space formula parameterizing all such controllers is obtained, where essential free parameters are constant matrices of fixed dimensions with a norm bound and a real number γ within a known interval.

d problem synthesis

The inner uncertainty (friction torque) and the outer uncertainty (wind disturbance) can be formed into a general feedback control system as shown in figure 6. Where, penalty signals w_2 and z_2 are used to guarantee the robustness of multiplicative oscillation, z_1 is the penalty signal of control input u, w_1 and z_1 is the penalty signals of wind disturbance response; W_3 describes the magnitude of multiplicative oscillation, W_4 represents the dynamic properties of wind disturbance, W_2 usually is chosen as a constant used to adjust the rate of response, W_1 is the penalty function used to modulate the magnitude of input signal. The $W_i, i = 1,2,3,4$ is finally given by:

$$W_1 = \frac{s+2.5}{s+5}$$

$$W_2 = 0.1$$

$$W_3 = \frac{s^2+s+570}{s^2+1.2s+402}$$

$$W_4 = \frac{4.39s+1}{s^2+0.789s+0.1556} \times 0.7434$$

The H_∞ synthesis problem consists of minimizing the eigenvalue of the generalized matrix of transfer function from inputs u and $w_i, i = 1,2$ to outputs θ_m and $z_i, i = 1,2,3$.

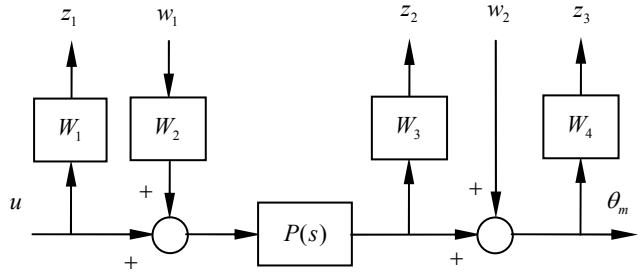

Fig.9 General control system of Alt-Az mounting

e simulation results

Figure 10 shows the 10th order H_∞ controller solved by MATLAB7.0. Further taking the wind oscillation as random noise, the azimuth and altitude tracking with velocity of 1 arcsec/s are shown in figure 11 and 12. The position errors of H_∞ controller with tracking speed 1arcsec/s are shown in figure 13and 14. From figure 13 and 14, the position errors have been obviously improved.

6. CONCLUSION

This paper has presented a design methodology for a high-accuracy motion control system with H_∞ controller in the presence of wind disturbance and friction oscillation. Servo controllers based on conventional feedback controller like PID controller are not effective for compensation of above mentioned two kinds of uncertainties. In order to minimize wind disturbance and friction oscillation, robust H_∞ controller was designed in this paper. The simulation results show that this technique can be better to meet the challenge presented to the servo control of LAMOST main axes.

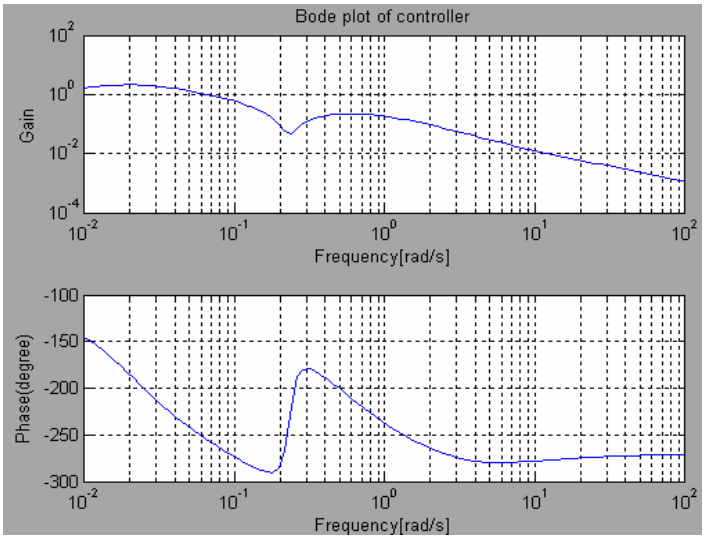

Fig .10 H_∞ controller

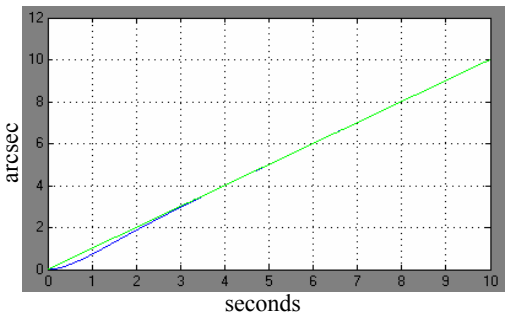

Fig.11 Azimuth tracking with H_∞ controller

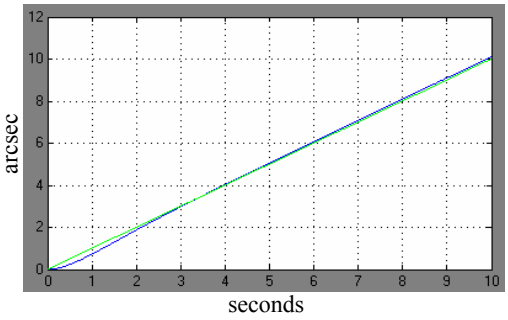

Fig.12 Altitude tracking with H_∞ controller

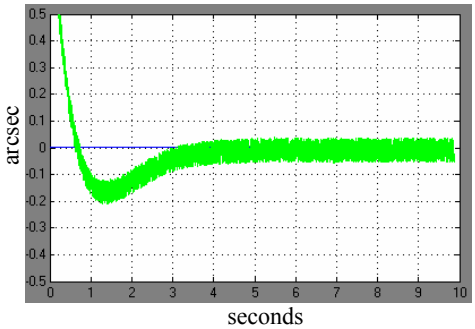

Fig.13 Position error curve of Azimuth (1arcsec/s)

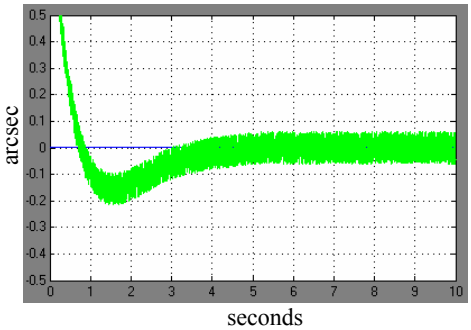

Fig.14 Position error curve of Altitude(1arcsec/s)

REFERENCES

[1] Kang M S. Robust Digital Friction Compensation. Control Engineering Practice. 1998, 6(3):359-367

[2] Development of a navel dynamic friction model and precise tracking control using adaptive back-stepping sliding mode controller. Mechatronics 16 (2006) 97-104

[3] Liu Qiang. Robust Nonlinear Friction Compensation of High Precision Servo System with Time Variable Parameters. Electro Transmission 2002,6:10-13

[4] C. Canudas De Wit, H. Olsson, K. J. Astrom, P. Lischinsky A new model for control systems with friction. IEEE Trans Automat Control 1995; 40: 419-425

[5] C. Canudas De Wit Comments on "A new model for control of systems with friction". IEEE Trans Automat Control 1998; 43: 1189-1190

[6] Gustavo A. Medrano-cerda, Robert D. Lett and Paul Rees H-Infinity motion control system for a 2 m telescope, proceeding of SPIE 2002; vol.4836: 88-97